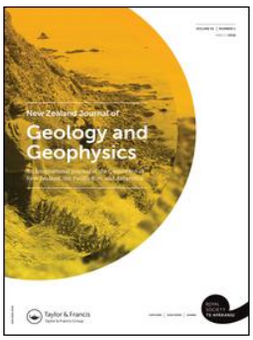

New Zealand Journal of Geology and Geophysics

ISSN: (Print) (Online) Journal homepage: https://www.tandfonline.com/loi/tnzg20

K-Ar fault-gouge dating in the Lower Buller gorge constrains the formation of the Paparoa Trough, West Coast, New Zealand

Uwe Ring , Ibrahim Tonguc Uysal , Kui Tong & Andrew Todd

To cite this article: Uwe Ring , Ibrahim Tonguc Uysal , Kui Tong & Andrew Todd (2020): K-Ar fault-gouge dating in the Lower Buller gorge constrains the formation of the Paparoa Trough, West Coast, New Zealand, New Zealand Journal of Geology and Geophysics, DOI: 10.1080/00288306.2020.1808025

To link to this article: https://doi.org/10.1080/00288306.2020.1808025

Published online: 19 Aug 2020.

NEW ZEALAND JOURNAL OF GEOLOGY AND GEOPHYSICS
https://doi.org/10.1080/00288306.2020.1808025

Taylor & Francis
Taylor & Francis Group

RESEARCH ARTICLE

OPEN ACCESS Check for updates

K-Ar fault-gouge dating in the Lower Buller gorge constrains the formation of the Paparoa Trough, West Coast, New Zealand

Uwe Ring [a], Ibrahim Tonguc Uysal[b,c], Kui Tong[c,d] and Andrew Todd [c]

[a]Department of Geological Sciences, Stockholm University Stockholm, Sweden; [b]Geological Engineering Department, Ankara University, Gölbaşı, Ankara, Turkey; [c]CSIRO Energy, Kensington, Australia; [d]State Key Laboratory of Oil and Gas Reservoir Geology and Exploitation, University of Technology, Chengdu, People's Republic of China

ABSTRACT

K-Ar dating of fault gouge from the intersection of the WNW-striking Ohika Detachment of the Paparoa Metamorphic Core Complex and a NNE-striking high-angle normal fault (Ohikaiti Fault) yielded an age of 103 ± 3.5 Ma (1σ uncertainty) for metamorphic white mica and an age of 35.2 ± 2.3 Ma for fault-gouge formation. The K-Ar four-point isochron is well defined and the upper-intercept age of 103 ± 3.5 Ma is inferred to reflect growth of metamorphic white mica in the footwall of the Paparoa Metamorphic Core Complex. We relate the fault gouge at the Ohikaiti Fault to the formation of the Paparoa Trough in the latest Eocene and the deposition of the Rapahoe Group. The NNE-striking Ohikaiti Fault either reactivated a favourably oriented segment of the Ohika Detachment or cut the detachment and displaced it when the Paparoa Trough formed. We discuss a model of relatively modest deformation in the Paparoa Trough as part of the Challenger Rift System because the northern West Coast region was close to the pole of plate rotation in the late Eocene and Oligocene.

ARTICLE HISTORY
Received 21 April 2020
Accepted 6 August 2020

HANDLING EDITOR
Phaedra Upton

KEYWORDS
Paparoa Range; South Island of New Zealand; fault-gouge dating; Faultslip analysis; Paparoa Trough; extensional defo

Introduction

The Austral Superprovince geological basement terranes of the New Zealand sector of the continent Zealandia (Figure 1a) had a complicated Meso/Cenozoic tectonic history involving various contractional and extensional episodes. The terranes were assembled in the Jurassic and Early Cretaceous on the paleo-Pacific margin of Gondwana (Mortimer 2004; Mortimer et al. 2017). Shortly after accretion, Zealandia began to extend and core complexes and various graben systems formed (Bradshaw 1989; Laird and Bradshaw 2004; Crampton et al. 2019). On the West Coast of the South Island, the various extension events and associated basin formation phases are variably preserved in rock exposures and through stratigraphic and structural relationships.

Alternating contractional and extensional deformation phases at multi-cycle continental margins remain a challenging problem for scholars aiming at resolving tectonic history. The extensional events on the West Coast since the mid-Cretaceous include the development of the mid-Cretaceous Paparoa Metamorphic Core Complex, a phase of Late Cretaceous to Paleocene basin formation, creating the Paparoa Basin, and post-Paleocene normal faulting and the development of the Paparoa Trough (Beggs et al. 2008). It appears that the mid-Cretaceous Paparoa Metamorphic Core Complex formed a marked anisotropy that has later been repeatedly exploited. All these basins were, at least in part, inverted by horizontal shortening associated with the Neogene Australian-Pacific plate boundary and the formation of the Southern Alps (Ghisetti and Sibson 2006).

Unravelling superimposed basin-forming events on the West Coast has been tackled with a variety of methods. Paleontologically defined ages of basin sediments have commonly and successfully been used to date basin formation (Nathan et al. 1986; Laird and Bradshaw 2004). Lever (2001) used a different approach mapping unconformity-bound sedimentary sequences. As unconformities represent hiatuses, they imply erosion, not deposition in the developing basin, and are thus an indirect approach. Seward and White (1992) applied fission-track cooling ages to constrain the timing of exhumation and footwall uplift at extensional faults. Schulte et al. (2014) took this approach a step further by combining low-temperature thermochronology with radiometric dating of extension-related mylonite in the footwall of the Paparoa Metamorphic Core Complex. A relatively recent and novel method for dating deformation structures in the brittle crust is K-Ar, $^{40}Ar/^{39}Ar$ and Rb-Sr dating of illite in fault gouge (Kralik et al. 1987; van der Pluijm et al. 2001) and this method has been applied to the Southern Alps (Ring et al. 2017a). An even newer method now coming into use is U-Pb calcite dating

CONTACT Uwe Ring uwe.ring@geo.su.se Department of Geological Sciences, Stockholm University, 10691 Stockholm, Sweden

of veins, fibres and striations (Ring and Gerdes 2016; Roberts and Walker 2016).

Another indirect way of analysing superimposed deformation is determining the kinematics of fault structures (Hancock 1985; Petit 1987), which provides a relative sequence of deformation events (Ghisetti & Sibson 2006; Ring et al. 2017b). Kinematic analysis of faulting can be combined with absolute age dating. Hansman et al. (2018) recently provided an example unravelling the absolute timing of three diagenetic and six brittle deformation events.

In this article, we combine kinematic analysis of faulting and fault-gouge dating in the lower Buller gorge. We collected a sample of fault gouge from the boundary between granite and gneiss of the Paparoa Metamorphic Core Complex and the tectonically overlying mid-Cretaceous Hawks Crag Breccia. In general, the fault gouge could be related to four events: (1) the development of the mid-Cretaceous Paparoa Metamorphic Core Complex; (2) Late Cretaceous to Paleocene basin formation; (3) post-Paleocene development of the Paparoa Trough; or (4) Miocene to Recent transpressional shortening across the Neogene Australian-Pacific plate boundary.

Geological background and setting

The basement of the South Island of New Zealand consists of several Paleozoic and Mesozoic terranes, which are grouped into the Eastern and the Western provinces (Figure 1) (Landis and Coombs 1967; Mortimer 2004). The Eastern Province mostly consists of Mesozoic accretionary complexes that formed along the paleo Pacific-Gondwana margin (Bradshaw 1989; Mortimer 2004; Adams et al. 2009). In contrast, the Western Province terranes represent fragments of the Paleozoic eastern continental margin of Gondwana (Cooper 1989; Mortimer 2004).

In the mid-Cretaceous, convergent margin tectonics in the proto-New Zealand part of the Gondwana margin came to an end and lithospheric extension commenced (Bradshaw 1989; Mortimer 2004). Extension started by 116 ± 6 Ma (Schulte et al. 2014) and core complexes formed along the rheologically soft magmatic arc of the subduction system (Figure 1a) (Tulloch and Kimbrough 1989; Kula et al. 2009; Ring et al. 2015). Continental extension along the West Coast of the South Island preceded the opening of the Tasman Sea at ~83 Ma (Gaina et al. 1998) by about 25–30 Myr (Schulte et al. 2014). The unroofing and elevation of the footwalls of the metamorphic cores led to the deposition of Motuan (~103–100 Ma; according the New Zealand Geological Timescale of Raine et al. 2015) basement-derived breccias (Tulloch and Palmer 1990) in adjacently developing WNW-trending half graben (Laird and Bradshaw 2004). Continental extension and the eventual separation of

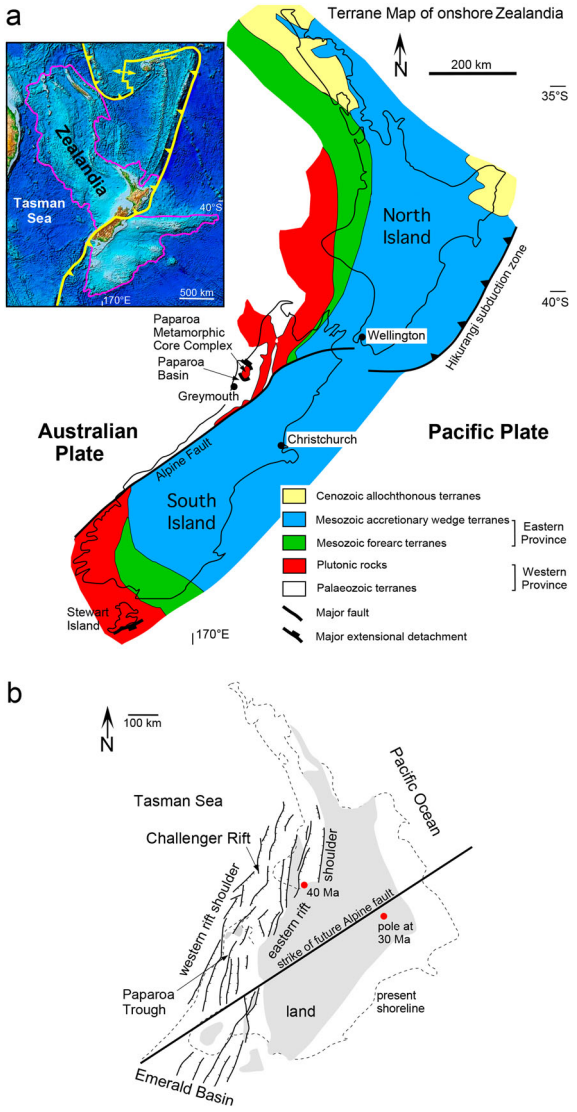

Figure 1. (a) Basement terrane map of New Zealand showing the Eastern and Western provinces, Paparoa Metamorphic Core Complex, and the Paparoa Basin at the southern end of the core complex. Inset shows New Zealand's North and South islands within Zealandia. (b) Oligocene Challenger Rift System through western New Zealand with outline of present shoreline and strike of future Alpine Fault for reference (modified from Kamp 1986a); also shown are rotation poles at 40 and 30 Ma according to King (2000) and the Paparoa Trough.

Australia and New Zealand was accompanied by alkaline magmatism between ~100 and 80 Ma (Laird 1994; Tulloch et al. 2009; van der Meer et al. 2018), with younger volcanics of this group coinciding with the formation of the Paparoa Basin near Greymouth and the SW-directed extensional reactivation of the Pike Detachment at the southern end of the Paparoa core complex at about 80–72 Ma (Schulte et al. 2014). Similar Late Cretaceous apatite fission-track ages occur in several other places in the South Island (Kamp 1997; Ring and Bernet 2010; Lang et al. 2018). Ring et al. (2018a) reported zircon fission-track ages of 79–46 Ma from the footwall of the Hyde-Macraes shear zone in the Otago Schist indicating NE-SW extensional reactivation. Bishop (1992) compiled nearly 400

orientations of Late Cretaceous lamprophyre dikes, revealing a prominent strike at 120°, compatible with NE-SW horizontal extension. Sedimentation in the graben systems resulting from NE-SW extension lasted until the late Paleocene and was accompanied by long-lasting deep-seated metamorphism (Cooper and Palin 2018; Briggs et al. 2018; Mortimer 2018; Ring et al. 2019). The extensional tectonism finally resulted in the emergence and erosion of the West Coast region in the Paleocene (Laird 1994; Lever 2001).

A major reorganisation of Zealandia tectonics took place in the Eocene with the termination of Tasman Sea spreading in the earliest Eocene (~55 Ma), the inception of the Pacific-Australian plate boundary and the opening of the small Emerald Basin to the south of New Zealand (Sutherland 1999) (Figure 1a). Seafloor spreading in the Emerald Basin commenced at around 45–40 Ma (Kamp 1986a; Sutherland 1999; King 2000). This process created the Challenger Rift System, a series of NNE-striking faults along the western side of New Zealand (Figure 1b) (Kamp 1986a). On the West Coast region, the Paparoa Trough close to the western shoulder of the Challenger Rift System developed in the Eocene (Nathan et al. 1986; Lever 2001). Kamp (1986b) showed that spatial and temporal tectonic patterns suggest that rifting in the South Island propagated northwards. The Paparoa Trough is situated close the late Eocene Pacific-Australia pole of plate rotation and by 38 Ma extension started to become oblique (Sutherland 1999; King 2000).

The magnitude of plate displacement within New Zealand during the period 45–25 Ma was small, but the displacement rate increased significantly after 25 Ma. This is due to migration of the instantaneous pole of Australia-Pacific rotation away from New Zealand (Sutherland 1999). The low rate between 45 and 25 Ma is well constrained because the pole of rotation during that time was very close to New Zealand (Sutherland 1999; King 2000; Furlong and Kamp 2009). Based on the age of dike swarms (Cooper et al. 1987), as well as patterns of changing sediment sources (King et al. 1999), the inception of the present-day Alpine Fault as a primarily strike-slip fault occurred by ~25 Ma (Kamp 1986b). The Alpine Fault dextrally offsets the terranes of the Eastern and Western provinces by ~460 km (Figure 1a). Currently, the Alpine Fault is the mid/upper-crustal expression of the Pacific-Australia plate boundary in the South Island (e.g. Norris et al. 1990).

Paparoa Range

The Paparoa Range is where the mid Cretaceous core-complex style extension and subsequent Late Cretaceous and post-Paleocene reactivation is best preserved and documented on the West Coast. In the mid-Cretaceous, the granitic and gneissic basement in the Paparoa Range was initially exhumed in the footwalls of a bivergent low-angle extensional fault system, forming the Paparoa Metamorphic Core Complex. The latter is bounded at its southern side by the top-SSW-displacing Pike Detachment and at its northern end by the top-NNE Ohika Detachment (Figure 2) (Tulloch and Kimborough 1989; Schulte et al. 2014). In the footwall of the Ohika Detachment, 110-Ma old, syn-tectonic granites intruded (Muir et al. 1997; Ireland and Gibson 1998). In the hanging wall of both detachments, the syn-extension Hawks Crag Breccia was deposited in WNW-trending half graben (Laird 1994).

The first reactivation of the Paparoa Metamorphic Core Complex is recorded by a second phase of cooling in the brittle crust in the footwall of the Pike Detachment at the southern end of the Paparoa Metamorphic Core Complex (Schulte et al. 2014) (Figure 1). The Pike Detachment was reactivated forming the Late Cretaceous to Paleocene Paparoa Basin (Nathan et al. 1986).

In the Paleocene, emergence and erosion resulted in peneplanation of the West Coast region (Laird 1994). Afterwards, a second phase of basin formation took place and the Paparoa Trough formed (Lever 2001). This second basin forming event is attributed to the NNE-ward propagation of the Challenger Rift System along the western side of New Zealand (Figure 1b) (Kamp 1986a) that created a series of NNE-striking, preferentially E-dipping normal faults. Hence, the geometry of these 'Challenger' basins was distinctly different from the previous extension events, which created WNW-trending basins. Rift-related sedimentation is recorded by the marine Rapahoe Group, which comprises an unconformity-bounded transgressive-regressive sequence (Lever 2001). Deposition of Rapahoe Group sediments occurred diachroneously across the basin from south to north during the Bortonian, Kaiatan, Runangan, and early Whaingaroan stages (approx. 43–33 Ma) (Laird 1988; Lever 2001). The sediments initially fine upwards from sandy, nearshore facies to more distal mud-dominated facies, and then coarsen upwards towards the early Whaingaroan upper unconformity, above which lie limestones of the Nile Group. The dominance of carbonate deposition and absence of significant terrigenous supply characterises tectonically largely undisturbed sedimentation during the Oligocene (Riordan et al. 2014). By the end of the Oligocene, large parts of Zealandia were below sea level (e.g. Mildenhall et al. 2014).

Vitrinite reflectance data indicate that during the Cenozoic the coastal part of the Paparoa Metamorphic Core Complex was buried distinctly less than the Paparoa Range itself (Nathan et al. 1986; Suggate 1959; Seward & White 1992; Kamp et al. 1999). Partially annealed apatite fission tracks indicate that burial in the Eocene and Oligocene Paparoa Trough was less

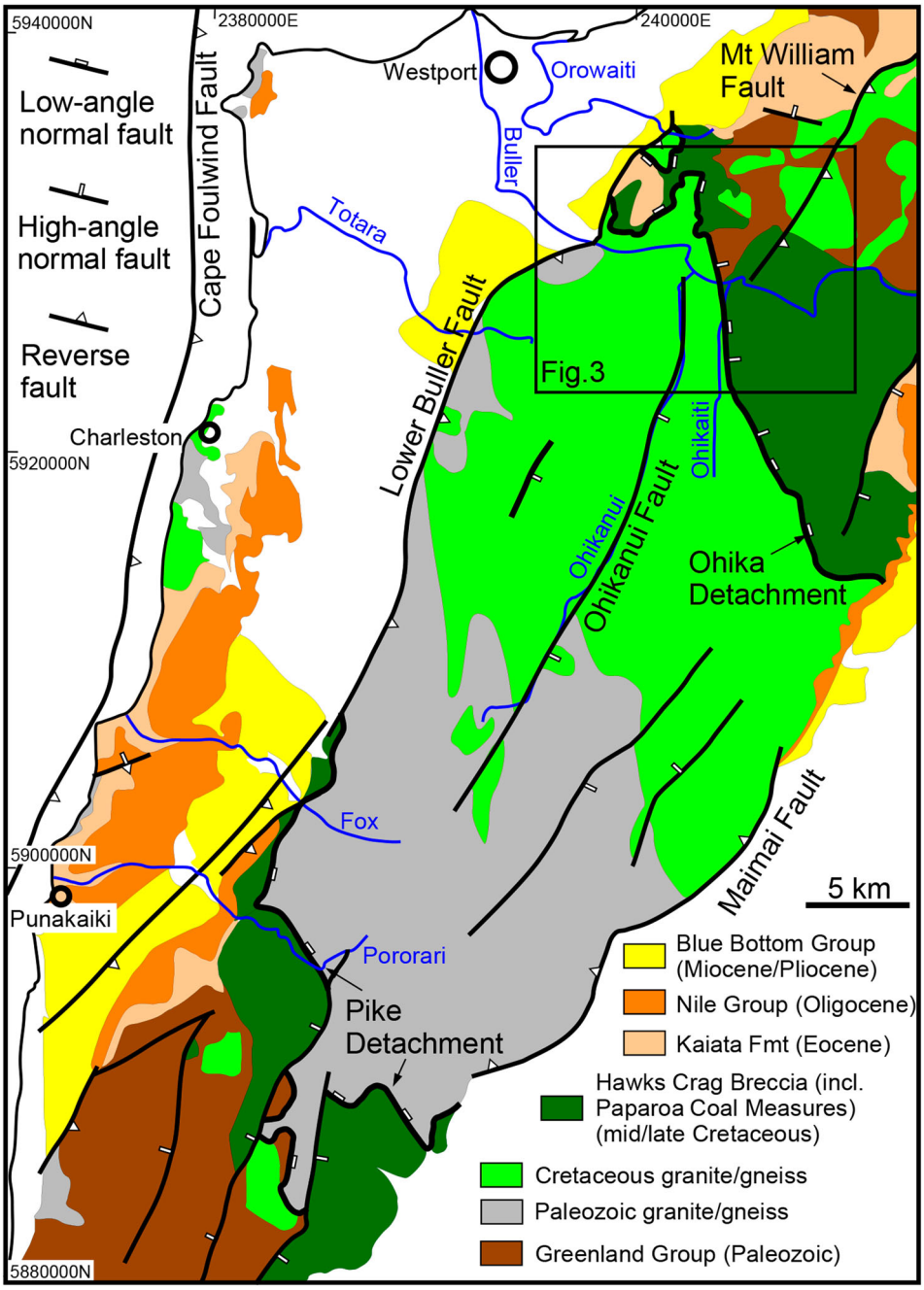

Figure 2. Tectonic map of the Paparoa Metamorphic Core Complex (modified from Nathan et al. 2002) showing the mid Cretaceous Ohika and Pike low-angle detachment faults, NNE-striking high-angle normal faults and shallower dipping Lower Buller and Maimai reverse faults (after Seward and White 1992; Ghisetti and Sibson 2006; Schulte et al. 2014). Map coordinates refer to New Zealand Map Grid which uses the New Zealand Geodetic Datum 1949.

than about 3 km (Seward and White 1992; Schulte et al. 2014).

Miocene to Recent transpressional shortening across the Australia-Pacific plate boundary has overprinted earlier structures to various degrees depending on how they were oriented relative to the Miocene to Recent stress field (Ghisetti and Sibson 2006). The young deformation is well preserved and better understood than previous, commonly overprinted deformation events (Findlay 1987; Holm et al. 1989; Batt et al. 2000; Ghisetti et al. 2016; Ring et al. 2019). This young shortening event re-exposed the Paparoa Range as a Miocene to Recent pop-up structure west of the Alpine Fault (Figure 1), bounded by the E-dipping reverse Lower Buller Fault on its western side and the associated W-dipping Inangahua and Maimai reverse faults in the east (Ghisetti and Sibson 2006) (Figure 2). Within the Paparoa Range, a few NNE-striking reverse faults occur (Figure 2). At the coastline between Westport and Greymouth, the lower plate of the Paparoa Metamorphic Core Complex is exposed as part of the hanging wall to the offshore E-dipping Cape Foulwind Fault (Figure 2).

While the timing of Late Cretaceous formation of the Paparoa Basin is reasonably well constrained (Seward and White 1992; Schulte et al. 2014), direct dating

of structures forming the Paparoa Trough is largely lacking and the timing of basin formation is constrained by the age of sediments that infill it (Nathan et al. 1986; Laird 1988; Rattenbury et al. 1998) and inferred from unconformities in the sedimentary succession (Lever 2001). The lack of structural information on the formation of the Paparoa Trough is because related extensional faults are severely overprinted by pervasive younger structures on the West Coast (Ghisetti and Sibson 2006). Fission-track thermochronology provided age constraints for the Late Cretaceous faulting in the southern Paparoa Range but apatite fission tracks show mixed age populations in the northern part of the range broadly indicating Cenozoic reactivation (Seward and White 1992; Schulte et al. 2014). Fault gouge containing newly-formed illite could help constraining the age of extensional deformation. However, fault gouge is hard to find on the West Coast due to intensive weathering and vegetation.

Methods

Sampling

Fault gouge was sampled near the contact between gneiss and granite of the Paparoa Metamorphic Core Complex and the tectonically overlying mid-Cretaceous Hawks Crag Breccia in a road ditch just west of Ohikaiti River (41°50'59"S, 171°43'49"E) where the low-angle Ohika Detachment strikes at 340–345° and is overprinted by the NNE-striking high-angle Ohikaiti fault (Figure 3). The Ohikaiti Fault is favourably oriented for having been reactivated during Miocene to Recent shortening. Therefore, the gouge could potentially be related to one of the four major tectonic events outlined above.

Kinematic analysis

To aid interpretation of the age derived from fault-gouge dating, we studied fault patterns in the Lower Buller gorge (Figure 3) and conducted a fault-slip analysis. Because of the poor outcrop conditions, severe weathering and limited accessibility in the Paparoa Range, a detailed fault-slip analysis was impossible. We have attempted to map at least 10 faults in each outcrop. However, this was usually not possible and we pooled measurements from various outcrops over an area of approximately 0.2–0.3 km^2 (Figure 3). In the caption to Figure 3 we briefly describe the fault pattern from each area, the main text describes aspects of the overall pattern in the Lower Buller gorge. More information on the kinematic analysis is provided in the supplementary material (https://doi.org/10.5281/zenodo.3970805).

Field work was conducted in the vicinity of major mapped faults (Figure 2) (Nathan et al. 2002). We mapped the orientations of 188 small-scale faults and associated striations (Figure 4). We focused on mesoscale fault planes associated with the map-scale faults. The displacement of the measured fault planes is generally in the range of centimetres to metres. The reason for relating these minor faults to the kinematic evolution of the mapped faults is their spatial relationship to them. The increasing number of secondary faults in the direct vicinity of the main faults implies a genetic link between the minor and the major faults. In the field, crosscutting relationships between faults and mutual offsets indicated successive slip events and the relative age of striae.

The brittle fault zones observed in outcrops are commonly penetratively fractured into arrays of blocks whose surfaces have different orientations. The cataclastic rocks associated with the faults have a rubbly to fragmental appearance and show numerous mesoscopic brittle faults, which are characterised by anastomosing clayey gouge layers with thin (~1 mm to 10 cm) zones of cataclasite, breccia and hematite-clay-coated fractured rock. Weakly oriented phacoid-shaped tectonic slivers of country rock in the fault zone are in the centimetre to decimetre range. Individual blocks are separated by thin, striated surfaces, which provide the direction of slip on fault planes (e.g. Hancock 1985; Petit 1987; Doblas 1998). We distinguish slickensides, striations, and slickenfibres. Slickensides is the planar, polished, surface of a fault plane. Striations (or slickenlines) are linear grooves scratched into fault surfaces by brittle wear and are the most common type of striae observed in the Lower Buller gorge. Slickenfibres comprise new minerals (mainly quartz, chlorite and epidote) precipitated on a fault surface as fibres elongated parallel to the slip vector.

At the outcrop scale, we recorded mainly faults with structures indicative of slip direction and shear sense. The sense of movement along the striae was inferred from kinematic indicators. Commonly used slip indicators were secondary fractures (Riedel shears), crescentic marks, asymmetric elevation, steps, and fibrous minerals (Petit 1987; Doblas 1998) (Figure 4). The Riedel shears caused lunate and crescentric structures at their intersections with the fault plane expressed as asymmetric steps subperpendicular to frictional-wear striations. The risers of the steps are generally incongruous. The mean fault plane is joined by repeated secondary striated fractures in secondary Riedel shear attitude dipping at a small angle to the wallrock. Their intersection with the mean fault plane is subperpendicular to the slip direction. The fault surface is often serrated in profile due to the intersection of two sets of secondary shears, syn- and antithetic Riedel shears (Petit 1987). The sub-planar, synthetic Riedel shears dip into the wallrock at an

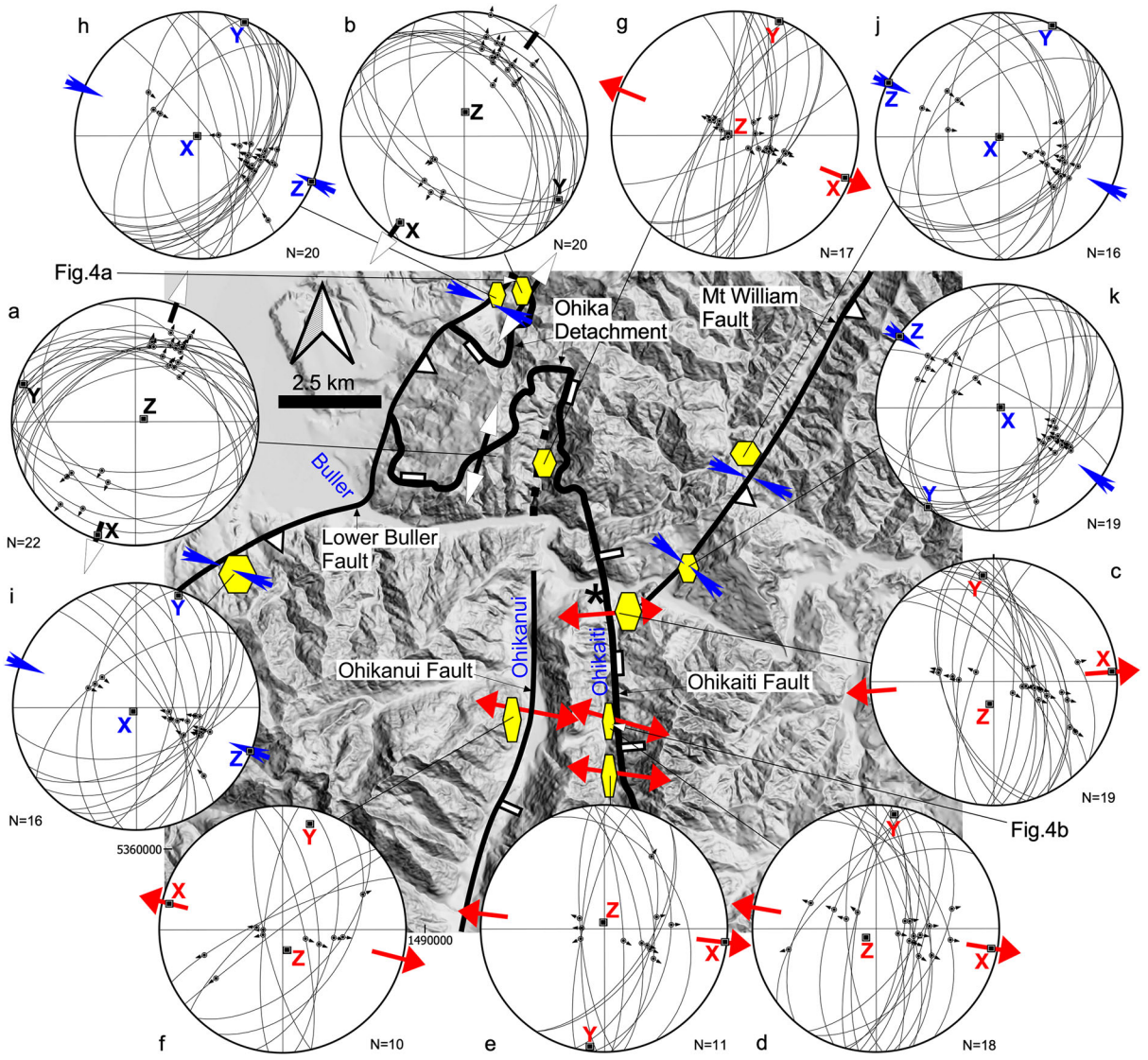

Figure 3. New Zealand 8-m digital elevation model (DEM) (data.linz.govt.nz/layer/768) of western Lower Buller gorge showing the fault pattern, the locality of sample PCC17-12 (black star) and the sites where the photos in Fig. 4 were taken. Black arrows with white arrow heads indicate mid/Late Cretaceous subhorizontal extension directions on low-angle Ohika Detachment; red arrows show sub-horizontal extension directions for NNE-striking high-angle normal faults and blue arrows indicate subhorizontal shortening directions for Miocene to Recent reverse faults. Note two types of ticks on Ohikaiti Fault illustrating normal reactivation of former low-angle detachment fault. (a-k) Fault-slip data. Diagrams show fault-plane great circles, poles for striations on the fault planes, arrows indicating hanging-wall slip direction, and principal strain axes (X > Y>Z). Note that the data were collected from scattered outcrops within an approximately 0.2–0.3 km^2 area indicated by the yellow polygons (the size of the polygons crudely reflects the area of observations). (a, b) Mainly shallowly NE-dipping fault planes with NNE-plunging striae providing NNE-SSW extension direction for the Ohika Detachment. (c-g) Sets of steep, about N-S-striking, conjugate normal faults indicative of WNE-ESE extension. (h-k) Mainly NNE-striking moderately to steeply dipping reverse faults proving WNW-ESE-trending shortening direction. Map coordinates refer to New Zealand Map Grid which uses the New Zealand Geodetic Datum 1949.

angle of 20–25°. P surfaces (Petit 1987) commonly formed at an even smaller angle to the fault plane but dip into the opposite direction than the Riedel shears.

Cresentric marks include stepped marks, plucking, gouging grain growth and tension gashes (Doblas 1998) (Figure 4). Asymmetric elevation features are knobby elevation (Figure 4a), which have their steep side facing into the opposite direction of the movement direction of the missing block.

Irregularities on the fault surface caused local crystallization of fibrous minerals, which produce steps (slickenfibres in Figure 4b). They appear as a set of steps (accretion steps) whose risers are sub-perpendicular to the striae and face in the same direction. These accretion steps are congruous, that is, risers facing towards the movement of the missing block (Petit 1987). Another frequent sense-of-slip indicator is quartz grown in dilatational fault-surface jogs.

Fibre and striae orientations on slickensides from the subsidiary faults in the mapping area are usually simple and consistent, and are interpretable with the geometry of the mapped faults at a regional scale. However, sometimes striae are not well developed or several

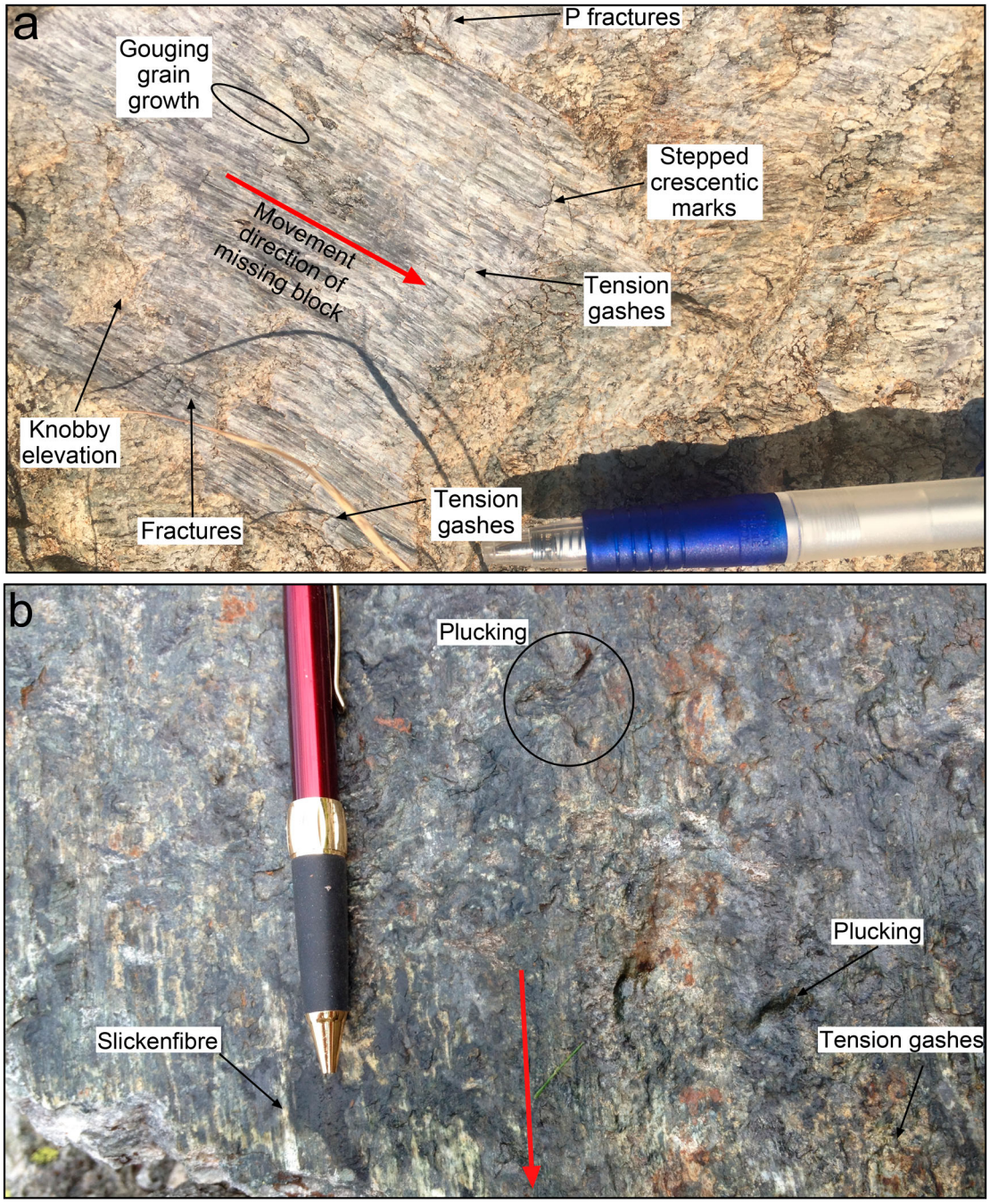

Figure 4. Outcrop photos of slickenside kinematic indicators. (a) Annotated fault surface with shallowly plunging slickensides in Buckland granite in the upper Orowaiti River. The various kinematic indicators and their interpretation are after Doblas (1998). (b) Steeply plunging striations in Buckland Granite in Ohikaiti valley. Note very fine-grained (blackish) fault surface with pluck marks (for localities from where pictures are taken see Fig. 3).

generations of striae are present. If interpretation of these complicated structures was too difficult or the structures were not interpretable, we discarded the measurements. Because all measurements were collected in basement rocks, only relative ages could be recorded.

Fault-gouge dating

Fault gouge generated in upper-crustal, brittle fault zones contains crushed rock fragments including metamorphic mica derived from the protoliths with variable amounts of newly-grown authigenic illite, which can be distinguished from each other by the type of crystallographic stacking, called polytypism (Verma and Krishna 1966). The $1M/M_d$ polytype is diagnostic of fault-related authigenic illite and commonly grows during the development of clay-rich gouge at temperatures less than 200°C (Grathoff et al. 2001). Fault gouge also contains higher temperature (>280°C) illite/muscovite, which is mechanically introduced into the gouge from the host rock and typically occurs as the $2M_1$ polytype (Srodon and Eberl 1984). The $2M_1$ polytype is indicative for metamorphic or magmatic

muscovite. The $1M/M_d$ polytype usually occurs as very fine-grained crystallites and is distinctly smaller than the detrital illite/muscovite $2M_1$ polytype. Therefore, the $1M/M_d$ polytype indicates in-situ growth in the gouge and is not an inherited phase (Vrolijk and van der Pluijm 1999; van der Pluijm et al. 2001). Radiogenic Ar is locked in the illite lattice as long as later fluid circulations or thermal events have not affected the samples at sufficiently high temperatures (close or higher than the illite formation temperature) assumed to cause partial or complete Ar loss (Clauer and Chaudhuri 1995; Lerman et al. 2007).

The absolute concentrations of the various polytypes can be quantified using X-ray diffraction (XRD) techniques and aliquots with different polytype ratios can be isotopically dated using the $^{40}Ar/^{39}Ar$, K-Ar or Rb-Sr methods (Kralik et al. 1987; van der Pluijm et al. 2001).

K–Ar dating was performed at the CSIRO Argon facility in Perth, Australia, according to standard methods detailed in Dalrymple and Lanphere (1969). The potassium content was determined by atomic absorption. The error of K determination of standards is better than 2.4% (2σ). The K blank was measured at 0.50 ppm. Argon was extracted from the separated mineral fraction by fusing the sample within a vacuum line serviced by an on-line ^{38}Ar spike pipette. The isotopic composition of the spiked Ar was measured with a high sensitivity, on-line VG3600 mass spectrometer. The ^{38}Ar was calibrated against standard biotite GA1550 (McDougall and Roksandic 1974). Blanks for the extraction line and mass spectrometer were systematically determined and the mass discrimination factor was determined periodically by airshots (small amounts of air for $^{40}Ar/^{36}Ar$ ratio measurement). During the course of the study, 16 international standards (eight HD-B1 and eight LP-6; Hess and Lippoldt 1994; Odin 1982) and 16 airshots were analysed. The error of the $^{40}Ar/^{36}Ar$ value of the airshot yielded 296.08 ± 2.4 (0.82%; 2σ). The general error for argon analyses is below 2.6% (2σ) based on the long-term precision of 330 measurements of international Ar standards. The K-Ar age was calculated using ^{40}K abundance and decay constants recommended by Steiger and Jäger (1977). The age uncertainties take into account the errors during sample weighing, $^{38}Ar/^{36}Ar$ and $^{40}Ar/^{38}Ar$ measurements and K analysis. Details of the XRD methodology and more information on K-Ar fault-gouge dating are provided in the supplementary material (https://doi.org/10.5281/zenodo.3970805).

Results

Fault kinematics

Figure 3 provides a generalised tectonic map of the Lower Buller gorge (Tulloch and Kimbrough 1989; Nathan et al. 2002; Schulte et al. 2014). The oldest and also major structure is the low-angle Ohika Detachment, which has been folded in the west by W-vergent tight to open folds with NNE-plunging fold axes (Nathan et al. 2002). The Ohika Detachment has been offset by a few NNE-striking high-angle faults. Ghisetti and Sibson (2006) showed that these faults have an older normal-slip component and were later, in part, reactivated as reverse faults.

Our sparse kinematic data indicate NNE-directed extension at the western Ohika Detachment (Figure 3a, b, 4a). Further east, the Ohika Detachment has a strike of 340–345° and in a few places, there are two sets of striations on fault surfaces. The first set is barely discernable, while the younger set of striations has a distinctly steeper plunge (Figure 3c-g). The high-angle faults cutting the Ohika Detachment also display down-dip striations. South of State Highway 6, scattered outcrops in the the Ohikaiti and Ohikanui rivers show a set of steeply plunging striations with normal-sense offsets (Figure 3c-g, 4b). Fault-slip analysis provides a subhorizontal WNW-ESE extension direction (Figure 3c-g). The Mt William Fault is thought to have been a late Paleogene normal fault (Laird and Hope 1968; Barry and MacFarlan 1988; Laird and Nathan 1988) but we could not unambiguously identify any striations recording early normal slip.

Our data also record reverse-slip movement on NE-striking faults (Figure 3h-k). The data from the Lower Buller and Mt William faults provide a WNW-ESE shortening direction. The data we collected are mostly from relatively steep (45–60°) fault planes; however, in some outcrops, we observed a few shallower (35–40°) dipping reverse faults. There are occasional striations associated with reverse-slip slip indicators along the Ohikanui Fault and the Ohika Detachment in the Ohikaiti valley but our observations are too few for any meaningful analysis.

Gouge data

The various clay size fractions provide apparent K-Ar ages of 98.1 ± 2.3 (0.5–2 μm), 88.7 ± 2 (0.2–0.5 μm), 80.5 ± 1.9 (0.1–0.2 μm) and 48.5 ± 1.1 Ma (<0.1 μm) (2σ errors) (Table 1). The percentage of detrital illite/

Table 1. K-Ar and XRD data for four grain-size fractions used for fault-gouge dating.

Sample	Grain size (μm)	K_2O (%)	$^{40}Ar_{rad}$ (%)	$^{40}Ar_{rad}$ (mol/g)	Age±2σ (Ma)
PCC-17-12	<0.1	5.58	93.3	4.76E-10	48.5±1.1
PCC-17-12	0.2–0.1	6.81	93.4	9.72E-10	80.5±1.9
PCC-17-12	0.5–0.2	6.76	97.2	1.067E-09	88.7±2
PCC-17-12	2–0.5	6.63	97.9	1.160E-09	98.1±2.3

muscovite ($2M_1$) is plotted against the K–Ar ages of the four analyses (Figure 5). The individual data plot along a well-defined linear regression line with a high degree of precision. The best-fit regression defines an upper-intercept $2M_1$ detrital illite/muscovite age of 103 ± 3.5 Ma and a lower-intercept $1M/M_d$ illite age of 35.2 ± 2.3 Ma (1σ uncertainty) (Figure 5).

The good linear relationship (mean squared weighted deviation, MSWD=0.86) between the percentage of inherited $2M_1$ illite/muscovite and the K-Ar ages of the various size fractions suggests that the analysed illite/muscovite comprises a mixture of two end-members—the two polytypes. Therefore, we can exclude inheritance of the $1M/M_d$ polytype illite from the wallrock and/or a post-tectonic overprint of K–Ar systematics due to later thermal or fluid flow events. Consequently, the crystallization of the $1M/M_d$ polytype of illite is interpreted to have occurred during fault-gouge formation (van der Pluijm et al. 2001) at 35.2 ± 2.3 Ma. The $2M_1$ illite age of 103 ± 3.5 Ma agrees reasonably well with the timing of metamorphism in the Paparoa Metamorphic Core Complex and the intrusion of Cretaceous granites. Schulte et al. (2014) reported a Rb-Sr age of 116 ± 6 Ma for amphibolite-facies mylonitization, and Sagar and Palin (2011) provided LA-ICP-MS U-Pb zircon ages of 118 ± 2 Ma and 107–105 ± 2 Ma for emplacement and metamorphism-deformation, respectively, of the Charleston Orthogneiss. Ireland and Gibson (1998) determined similar U–Pb zircon and Th–Pb monazite ages for Charleston Orthogneiss emplacement (119 ± 2 Ma) and metamorphism (109 ± 5 Ma and 112 ± 2 Ma). Muir et al. (1997) reported a SHRIMP U-Pb zircon age 109.6 ± 1.7 Ma, Ireland and Gibson (1998) a Th-Pb monazite age of 111 ± 1.5 Ma, and Buchwaldt et al. (2011) CA-ID-TIMS ages ranging between 110.2 ± 0.2 Ma and 109.9 ± 0.1 Ma for emplacement of the Buckland Granite.

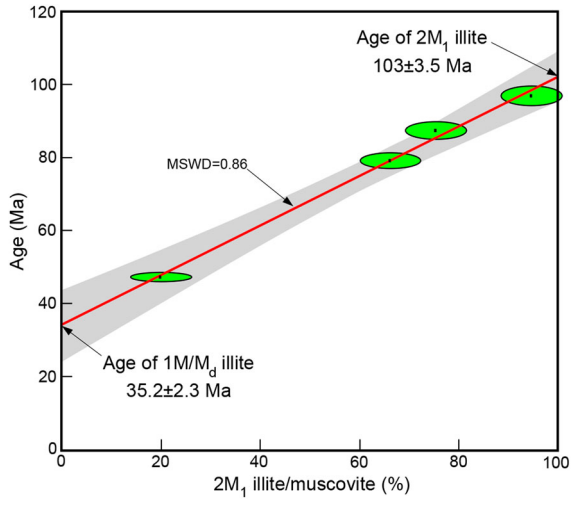

Figure 5. K-Ar ages of four grain-size fractions versus their proportion of $2M_1$ illite/muscovite for sample PCC 17–12 (see also Table 1). The relationship between K-Ar age and the $2M_1$ polytype is well-described by the linear regression (red line) with an upper-intercept age of 103 ± 3.5 Ma and a lower-intercept, gouge-formation age of 35.2 ± 2.3 Ma (1σ errors; note that the errors on the four ages for the various grain-size fractions are 2σ errors). The shaded areas either side of the red line show 68% confidence intervals (York et al. 2004; Vermeesch 2018).

Discussion

The most straightforward interpretation of the 35.2 ± 2.3 Ma fault gouge age is that it records faulting related to late Eocene extension and associated formation of the Paparoa Trough. Given its location at the intersection of the Ohikaiti Fault and the Ohika Detachment, the gouge could be related to (1) the formation of the Ohikaiti Fault, or (2) to oblique-normal reactivation of the Ohika Detachment. Option (1) would envisage a relatively straight, about WNW-striking Ohika Detachment that was not favourably oriented for late Eocene WNW-ESE extension and the new Ohikaiti Fault cut and downfaulted the Ohika Detachment. Because the detachment was shallowly N-dipping an apparent dextral displacement in map view results (Figure 6a). The Ohikaiti Fault would then be a newly formed fault that had no precursor structure.

Option (2) envisages that the WNW-striking Ohika Detachment was folded about NNE-trending axes during low-angle extensional shearing. Such folding with axes parallel to the tectonic transport direction is common in regions of large-scale continental extension, for example, the Basin-and-Range province (Coney 1980; Spencer 1984) and the Aegean Sea region (Isik et al. 2004; Gessner et al. 2013; Ring et al. 2018b), and also at oceanic core complexes (Tucholke et al. 1998). The limbs of such large-scale folds would be favourably oriented for late Eocene extensional reactivation and the Ohikaiti Fault formed in an E-dipping fold limb (Figure 6b).

It is hard to decide which option is more likely. We tentatively favour option (2) because there are relic detachment-related low-angle faults in scattered outcrops in the Ohikaiti valley. The folding in the western segment of the Ohika Detachment might be regarded as an original mid-Cretaceous extension-related fold structure. The Pike Detachment in the southern Paparoa Range also shows folding about SSW-plunging, tectonic-transport-parallel axes (Schulte et al. 2014). One could argue that in some places NNE-striking faults developed in the limbs of some of these folds.

We relate the fault-gouge age of 35.2 ± 2.3 Ma to the formation of the Paparoa Trough. Accordingly, we suggest that the Challenger Rift had propagated northwards into the Paparoa region by the latest Eocene-earliest Oligocene. Despite the error, this age is resolvably younger than the onset of seafloor spreading at about 45–40 Ma in the Emerald basin to the south of New Zealand and consistent with the idea that extensional

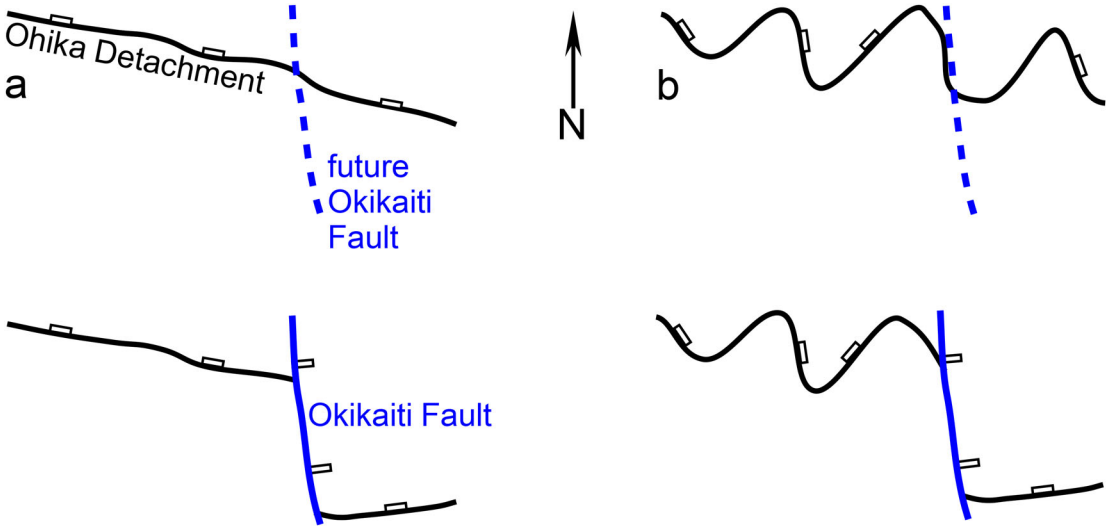

Figure 6. Two possible map interpretations for latest Eocene normal faulting in the Lower Buller gorge. (a) Relatively straight, approximately WNW-striking Ohika Detachment that was not favourably oriented for late Eocene WNW-ESE extension cut and downfaulted by the new Ohikaiti Fault. (b) WNW-striking Ohika Detachment that was folded about NNE-trending axes during mid/Late Cretaceous low-angle extensional shearing. The Ohikaiti Fault formed along one of the fold limbs favourably oriented for Eocene ENE-directed extension.

deformation in the South Island propagated from south to north (Kamp 1986a, 1986b). The age overlaps with the upwards coarsening trend of the sediments of the rift-related Rapahoe below the early Whaingaroan upper unconformity (Lever 2001). Limestone deposition in the Oligocene reflects tectonically rather undisturbed conditions that lead to widespread drowning of New Zealand by the end of the Oligocene (Mildenhall et al. 2014; Riordan et al. 2014). Our interpretation emphasises a rather short-lived (<10 Myr) phase of extensional deformation in the Paparoa Trough probably reflecting limited deformation in the northwestern South Island due to its proximity to the Australia-Pacific plate rotation pole at that time (King 2000).

A question would be how the Oligocene to Miocene apatite fission-track ages relate to latest Eocene-earliest Oligocene normal faulting? The obvious interpretation is that the apatite fission-track ages reflect footwall cooling following the inception of normal faulting. Such a view would be in line with the increase in mean track lengths of the apatite fission tracks 10–12 km east of the Lower Buller Fault (Seward and White 1992) as this is about the distance between the fault-gouge locality and the Lower Buller Fault. Also, the Ohika Detachment/Ohakaiti Fault is E-dipping and its reactivation would have (re)exhumed the Paparoa Metamorphic Core Complex leading to cooling of the footwall. However, Schulte et al. (2014) showed that samples with apatite fission-track ages between 34.5 ± 9.8 and 23.7 ± 6.6 Ma (2σ errors) fail the χ2-test, indicating that they have been partially reset by a later heating event. Seward and White (1992) already came to a similar conclusion in proposing that ages >20 Ma have negatively-skewed track-length distributions suggestive of partial annealing. Therefore, it appears more probable that the Oligocene and Miocene apatite fission track ages are mixed ages resulting from post-late Eocene burial followed by erosional exhumation (cooling) since the middle Miocene.

Conclusions

We dated fault gouge in the Lower Buller gouge at 35.2 ± 2.3 Ma and relate the age to faulting at the Ohakaiti Fault and the formation of the Paparoa Trough. The age agrees well with a coarsening upwards trend in sedimentation of the Rapahoe Group. We suggest that the period of basin development and the formation of the Paparoa Trough was a rather short-lived event (>10 Ma) near the Eocene/Oligocene boundary.

Acknowledgements

We thank Igor Villa, Johannes Glodny and Robert Bolhar for geochronological advice and Reuben Hansman and Hagen Deckert for discussing the fault-slip data. We thank Matt Sagar and an anonymous reviewer for detailed comments on the manuscript. UR acknowledges funding by the Swedish Research Council (Vetenskapsrådet, 2016-03461) and the Swedish Wenner-Gren Stiftelserna (SSh2018-0003).

Disclosure statement

No potential conflict of interest was reported by the author(s).

Data availability statement

The supplementary data are openly available at https://doi.org/10.5281/zenodo.3970805.

ORCID

Uwe Ring http://orcid.org/0000-0003-3347-9284
Andrew Todd http://orcid.org/0000-0001-5751-1301

References

Adams CJ, Mortimer N, Campbell HJ, Griffin WL. 2009. Age and isotopic characterisation of metasedimentary rocks from the Torlesse Supergroup and Waipapa Group in the central North Island, New Zealand. New Zealand Journal of Geology and Geophysics. 52:149–170. doi:10.1080/00288300909509883.

Barry J, MacFarlan D. 1988. Geology and coal resources of the Upper Waimangaroa and Mt. William South Sectors. Coal geology report 13. Wellington: Ministry of Energy.

Batt GE, Braun J, Kohn BP, McDougall I. 2000. Thermochronological analysis of the dynamics of the Southern Alps, New Zealand. Geological Society of America Bulletin. 112(2):250–266. doi:10.1130/0016-7606.

Beggs JM, Ghisetti FC, Tulloch AJ. 2008. Basin and petroleum systems analysis of the West Coast region, South Island, New Zealand. In: Bevin JE, Bradshaw BE, Uruski C, editor. Eastern Australasian Basins Symposium, Volume III. Sydney: PESA; p. 341–348.

Bishop DJ. 1992. Extensional tectonism and magmatism during the middle Cretaceous to Paleocene, North Westland, New Zealand. New Zealand Journal of Geology and Geophysics. 35(1):81–91. doi:10.1080/00288306.1992.9514502.

Bradshaw JD. 1989. Cretaceous geotectonic patterns in the New Zealand region. Tectonics. 8:803–820. doi:10.1029/TC008i004p00803.

Briggs S, Cottle J, Smit M. 2018. Record of plate boundary metamorphism during Gondwana breakup from Lu-Hf garnet geochronology of the Alpine Schist, New Zealand. Journal of Metamorphic Geology. 36(7):821–841. doi:10.1111/jmg.12313.

Buchwaldt R, Ring U, Tulloch AJ. 2011., Decoding the timing within the Paparoa Metamorphic Core Complex, New Zealand: new insights of the break-up of southern Gondwana. Geological Society of America Abstracts with Programs. 43(5):653.

Clauer N, Chaudhuri S. 1995. Clays in crustal environments. Isotope dating and tracing. Heidelberg: Springer. 359 p.

Coney PJ. 1980. Cordilleran metamorphic core complexes; an overview. In: Crittenden MDJ, Coney PJ, Davis GH ed. Cordilleran metamorphic core complexes. Geological Society of America Memoirs. 153:7–31.

Cooper RA. 1989. Early Paleozoic terranes of New Zealand. Journal of the Royal Society of New Zealand. 19(1):73–112.

Cooper AF, Barreiro BA, Kimbrough DL, Mattinson JM. 1987. Lamprophyre dike intrusion and the age of the Alpine fault, New Zealand. Geology. 15(10):941–944. doi:10.1130/0091-7613(1987)15<941:LDIATA>2.0.CO;2.

Cooper AF, Palin JM. 2018. Two-sided accretion and polyphase metamorphism in the Haast Schist belt, New Zealand: constraints from detrital zircon geochronology. Geological Society of America Bulletin. 130(9-10):1501–1518. doi:10.1130/B31826.1.

Crampton JS, Mortimer N, Bland KJ, Strogen DP, Sagar MW, Hines BR, King PR, Seebeck H. 2019. Cretaceous termination of subduction at the Zealandia margin of Gondwana: The view from the paleo-trench. Gondwana Research. 70:222–242.

Dalrymple GB, Lanphere MA. 1969. Potassium-argon dating: Principles, techniques and applications to geochronology. Techniques and Applications to Geochronology. San Francisco: WH Freeman and Company. 258p.

Doblas M. 1998. Slickenside kinematic indicators. Tectonophysics. 295:187–197.

Findlay RH. 1987. Structure and interpretation of the Alpine schists in Copland and Cook River Valleys, South Island, New Zealand. New Zealand Journal of Geology and Geophysics. 30(2):117–138. doi:10.1080/00288306.1987.10422178.

Furlong KP, Kamp PJJ. 2009. The lithospheric geodynamics of plate boundary transpression in New Zealand: Initiating and emplacing subduction along the Hikurangi margin, and the tectonic evolution of the Alpine Fault system. Tectonophysics. 474:449–462. doi:10.1016/j.tecto.2009.04.023.

Gaina C, Müller DR, Royer J-Y, Stock J, Hardebeck J, Symonds P. 1998. The tectonic history of the Tasman Sea: A puzzle with 13 pieces. Journal of Geophysical Research: Solid Earth. 103(B6):12413–12433. doi:10.1029/98JB00386.

Gessner K, Gallardo LA, Markwitz V, Ring U, Thomson SN. 2013. What caused the denudation of the Menderes Massif: review of crustal evolution, lithosphere structure, and dynamic topography in southwest Turkey. Gondwana Research. 24:243–274. doi:10.1016/j.gr.2013.01.005.

Ghisetti FC, Sibson RH. 2006. Accommodation of compressional inversion in north-western South Island (New Zealand): Old faults versus new? Journal of Structural Geology. 28:1994–2010. doi:10.1016/j.jsg.2006.06.010.

Ghisetti F, Sibson RH, Hamling I. 2016. Deformed Neogene basins, active faulting and topography in Westland: Distributed crustal mobility west of the Alpine Fault transpressive plate boundary (South Island, New Zealand). Tectonophysics. 693:340–362. doi:10.1016/j.tecto.2016.03.024.

Grathoff GH, Moore DM, Hay RL, Wemmer K. 2001. Origin of illite in the lower Paleozoic of the Illinois basin: evidence for brine migrations. Geology Society of America Bulletin. 113:1092–1104.

Hancock PL. 1985. Brittle microtectonics: Principles and practice. Journal of Structural Geology. 7:437–457.

Hansman RJ, Roper A, Gerdes A, Ring U. 2018. Absolute ages of multiple generations of brittle structures by U-Pb dating of calcite. Geology. 46:207–210. doi.org/10.1130/G39822.1.

Hess JC, Lippoldt HJ. 1994. Compilation of K-Ar measurements on HD-B1 standard biotite. In: Odin GS, editor. Phanerozoic time scale. Paris: Bull. Lias. Inform., IUGS subcom. Geochronol., 12; p. 19–23.

Holm DK, Norris RJ, Craw D. 1989. Brittle and ductile deformation in a zone of rapid uplift: Central Southern Alps, New Zealand. Tectonics. 8(2):153–168. doi:10.1029/TC008i002p00153.

Ireland TR, Gibson GM. 1998. SHRIMP monazite and zircon geochronology of high-grade metamorphism in New Zealand. Journal of Metamorphic Geology. 16:149–167.

Isik V, Tekeli O, Seyitoglu G. 2004. The 40Ar/39Ar age of extensional ductile deformation and granitoid intrusion in the northern Menderes core complex: implications for the initiation of extensional tectonics in western Turkey. Journal of Asian Earth Sciences. 89:757–765.

Kamp PJJ. 1986a. Relationship of the West Coast, North Island, igneous bodies to the mid-Cenozoic Challenger Rift System and subduction of the Pacific plate. New Zealand Journal of Geology and Geophysics. 29:51–60.

Kamp PJJ. 1986b. The mid-cenozoic Challenger Rift System of western New Zealand and its implications for the age of Alpine fault inception. Geological Society of America Bulletin. 97:255–281. doi:10.1130/0016-7606(1986)97<255:TMCRSO>2.0.CO;2.

Kamp PJJ. 1997. Paleogeothermal gradient and deformation style, Pacific front of the Southern Alps Orogen: constraints from fission track thermochronology. Tectonophysics. 271(1-2):37–58. doi:10.1016/S0040-1951(96)00246-6.

Kamp PJJ, Whitehouse IWS, Newman J. 1999. Constraints on the thermal and tectonic evolution of Greymouth coalfield. New Zealand Journal of Geology and Geophysics. 42:447–467.

King P. 2000. Tectonic reconstructions of New Zealand: 40 Ma to the present. New Zealand Journal of Geology and Geophysics. 43:611–638.

King PR, Naish TR, Browne GH, Field BD, Edbrooke SW. 1999. Cretaceous to Recent sedimentary patterns in New Zealand, Institute of geological & nuclear sciences folio series 1. Lower Hutt: Institute of Geological & Nuclear Sciences.

Kralik M, Klima K, Riedmüller G. 1987. Dating fault gogues. Nature. 327:315–317.

Kula J, Tulloch AJ, Spell TL, Wells ML, Zanetti KA. 2009. Thermal evolution of the Sisters Shear Zone, southern New Zealand: formation of the Great South Basin and onset of Pacific-Antarctic spreading. Tectonics. 28:1–22.

Laird M. 1988. Sheet S37 - Punakaiki. Geological map of New Zealand 1:63,360, Technical report, Department of Scientific and Industrial Research, Wellington.

Laird MG. 1994. Geological aspects of the opening of the Tasman Sea Basin. In: Van Lingen GJ, Swanson K, Muir RJ, editor. The evolution of the Tasman Sea basin. Rotterdam: Balkema; p. 1–17.

Laird MG, Bradshaw JD. 2004. The break-up of a long-term relationship: the Cretaceous separation of New Zealand from Gondwana. Gondwana Research. 7:273–286. doi:10.1016/S1342-937X(05)70325-7.

Laird MG, Hope JM. 1968. The Torea Breccia and the Papahaua overfold. New Zealand Journal of Geology and Geophysics. 11:418–434.

Laird MG, Nathan S. 1988. The Eocene Torea Breccia, S.W. Nelson: redescription, sedimentology, and regional significance. New Zealand Geological Survey Record. 35:104–108.

Landis CA, Coombs DS. 1967. Metamorphic Belts and Orogenesis in Southern New Zealand. Tectonophysics. 4:501–518.

Lang KA, Ehlers TA, Kamp PJJ, Ring U. 2018. Sediment storage in the Southern Alps of New Zealand: new observations from tracer thermochronology. Earth and Planetary Science Letters. 493:140–149. doi:10.1016/j.epsl.2018.04.016.

Lerman A, Ray BM, Clauer N. 2007. Radioactive production and diffusional loss of radiogenic ^{40}Ar in clays in relation to its flux to the atmosphere. Chemical Geology. 243:205–224.

Lever H. 2001. An Eocene to early Oligocene unconformity-bounded sequence in the Punakaiki-Westport area, West Coast, South Island, New Zealand. New Zealand Journal of Geology and Geophysics. 44:355–363.

McDougall I, Roksandic Z. 1974. Total Fusion ^{40}Ar/^{39}Ar ages using HIFAR reactor. Journal of the Geological Society of Australia. 21:81–89.

Mildenhall DC, Mortimer N, Bassett KN, Kennedy EM. 2014. Oligocene paleogeography of New Zealand: maximum marine transgression. New Zealand Journal of Geology and Geophysics. 57(2):107–109. doi:10.1080/00288306.2014.904387.

Mortimer N. 2004. New Zealand's Geological Foundations. Gondwana Research. 7:261–272.

Mortimer N. 2018. Evidence for a pre-eocene proto-alpine fault through Zealandia. New Zealand Journal of Geology and Geophysics. 61(3):251–259. doi:10.1080/00288306.2018.1434211.

Mortimer N, Campbell HJ, Tulloch AJ, King PR, Stagpoole VM, Wood RA, Rattenbury MS, Sutherland R, Adams CJ, Collot J, Seton M. 2017. Zealandia – Earth's hidden continent. GSA Today. 27:27–35. doi:10.1130/GSATG321A.1.

Muir RJ, Ireland TR, Weaver SD, Bradshaw JD, Waight TE, Jongens R, Eby GN. 1997. SHRIMP U-Pb geochronology of Cretaceous magmatism in northwest Nelson-Westland, South Island, New Zealand. New Zealand Journal of Geology and Geophysics. 40:453–463. doi:10.1080/00288306.1997.9514775.

Nathan S, Anderson HJ, Cook RA, Herzer RH, Hoskins RH, Raine JI, et al. 1986. Cretaceous and Cenozoic sedimentary basins of the West Coast region, South Island, New Zealand. New Zealand Geological Survey basin studies 1. Wellington, SIPC and DSIR. 89 p.

Nathan S, Rattenbury MS, Suggate RP. 2002. Geology of the Greymouth area (compilers). Institute of Geological and Nuclear Sciences. Geological Map 12, scale 1:250 000.

Norris RJ, Koons PO, Cooper AF. 1990. The obliquely-convergent plate boundary in the South Island of New Zealand: implications for ancient collision zones. Journal of Structural Geology. 12:715–725.

Odin GS, et al. 1982. Interlaboratory standards for dating purposes. In: Odin GS, editor. Numerical dating in stratigraphy. part 1. Chichester: John Wiley & Sons; p. 123–148.

Petit J-P. 1987. Criteria for the sense of movement on fault surfaces in brittle rocks. Journal of Structural Geology. 9(5/6):597–608.

Raine JI, Beu AG, Boyes AF, Campbell HJ, Cooper RA, Crampton JS, Crundwell MP, Hollis CJ, Morgans HEG, Mortimer N. 2015. New Zealand Geological Timescale NZGT 2015/1. New Zealand Journal of Geology and Geophysics. 58:398–403.

Rattenbury MS, Cooper RA, Johnston MR. 1998. Geology of the Nelson area: Institute of Geological & Nuclear Science 1:250 000 geological map 9. 1 sheet + 67 p: Institute of Geological & Nuclear Sciences Limited.

Ring U, Bernet M. 2010. Fission-track analysis un ravels the denudation history of the Bonar Range in the footwall of the Alpine Fault, South Island, New Zealand. Geological Magazine. 147:801–813. doi:10.1017/S0016756810000208.

Ring U, Gerdes A. 2016. Kinematics of the Alpenrhein-Bodensee graben system in the Alps: Tertiary extension due to the formation of the western Alps arc. Tectonics. 35:1367–1391. doi:10.1002/2015TC004085.

Ring U, Gessner K, Thomson SN. 2017b. Variations in fault-slip data and cooling history reveal corridor of heterogeneous backarc extension in the eastern Aegean Sea region. Tectonophysics. 700–701:108–130. doi:10.1016/j.tecto.2017.02.013.

Ring U, Glodny J, Angiboust S, Little T, Lang KA. 2019. Middle to late Miocene age for the end of amphibolite-facies mylonitization of the Alpine Schist, New Zealand: implications for onset of transpression across the Alpine fault. Tectonics. 38. doi:10.1029/2019TC005577.

Ring U, Glodny J, Peillod A, Skelton A. 2018b. The timing of high-temperature conditions and ductile shearing in the footwall of the Naxos extensional fault system, Aegean Sea, Greece. Tectonophysics. 745:366–381. doi:10.1016/j.tecto.2018.09.001.

Ring U, Mortimer N, Butz C, Bernet M. 2018a. Extensional deformation along the footwall fault below the Hyde-macraes Shear Zone, Otago Schist, New Zealand. New Zealand Journal of Geology and Geophysics. 61:219–236. doi:10.1080/00288306.2018.1467471.

Ring U, Tulloch A, Bernet M. 2015. Kinematic, finite strain and vorticity analysis of the sisters Shear Zone, Stewart Island, New Zealand. Journal of Structural Geology. 73:114–129. doi:10.1016/j.jsg.2015.02.004.

Ring U, Uysal IT, Glodny J, Cox SC, Little T, Thomson SN, et al. 2017a. Fault-gouge dating in the Southern Alps, New Zealand. Tectonophysics. 717:321–338.

Riordan NK, Reid CM, Bassett KN, Bradshaw JD. 2014. Reconsidering basin geometries of the West Coast: the influence of the Paparoa Core Complex on Oligocene Rift Systems. New Zealand Journal of Geology and Geophysics. 57(2):170–184. doi:10.1080/00288306.2014.904386.

Roberts NMW, Walker RJ. 2016. U-Pb geochronology of calcite-mineralized faults: absolute timing of rift-related fault events on the northeast Atlantic margin. Geology. 44:531–534. doi:10.1130/G37868.1.

Sagar MW, Palin M. 2011. Emplacement, metamorphism, deformation and affiliation of mid-Cretaceous orthogneiss from the Paparoa Metamorphic Core Complex lower-plate, Charleston, New Zealand. New Zealand Journal of Geology and Geophysics. 54:273–289. doi:10.1080/00288306.2011.562904.

Schulte DO, Ring U, Thomson SN, Glodny J, Carrad H. 2014. Two-stage development of the Paparoa Metamorphic Core Complex, West Coast, South Island, New Zealand: Hot continental extension precedes sea-floor spreading by ~25 my. Lithosphere. 6(3):177–194. doi:10.1130/L348.1.

Seward D, White PJ. 1992. Evolution and eversion of a tertiary sedimentary basin, Paparoa Range, West Coast, South Island, New Zealand: Evidence from fission-track dating. New Zealand Journal of Geology and Geophysics. 35:265–271. doi:10.1080/00288306.1992.9514520.

Spencer JE. 1984. Role of tectonic denudation in warping and uplift of low-angle normal faults. Geology. 12:95–98. doi:10.1130/0091-7613(1984)12 <95:ROTDIW>2.0.CO;2.

Srodon J, Eberl DD. 1984. Illite. In: Bailey W, editor. Reviews in Mineralogy, 13. Mineralogical Society of America; p. 495–544.

Steiger RH, Jäger E. 1977. Subcommission on geochronology: convention on the use of decay constants in geo- and cosmochronology. Earth and Planetary Science Letters. 36:359–362.

Suggate RP. 1959. New Zealand coals. New Zealand Department of Scientific and Industrial Research Bulletin. 134:113.

Sutherland R. 1999. Cenozoic bending of New Zealand basement terranes and Alpine Fault displacement: a brief review. New Zealand Journal of Geology and Geophysics. 42:295–301.

Tucholke BE, Lin J, Kleinrock MC. 1998. Megamullions and mullion structure defining oceanic metamorphic core complexes on the Mid-Atlantic Ridge. Journal of Geophysical Research: Solid Earth. 103:9857–9866. doi:10.1029/98JB00167.

Tulloch AJ, Kimbrough DL. 1989. The Paparoa Metamorphic Core Complex, New Zealand: Cretaceous extension associated with fragmentation of the Pacific margin of Gondwana. Tectonics. 8(6):1217–1234. doi:10.1029/TC008i006p01217.

Tulloch AJ, Palmer K. 1990. Tectonic implications of granite cobbles from the mid-Cretaceous Pororari Group, south-west Nelson, New Zealand. New Zealand Journal of Geology and Geophysics. 33:205–217.

Tulloch AJ, Ramezani J, Mortimer N, Mortensen J, Van Den Bogaard P, Maas R. 2009. Cretaceous felsic volcanism in New Zealand and Lord Howe Rise (Zealandia) as a precursor to final Gondwana break-up. Geological Society, London, Special Publications. 321:89–118.

van der Meer QHA, Waight TE, Tulloch AJ, Whitehouse MJ, Andersen T. 2018. Magmatic evolution during the cretaceous transition from subduction to continental break-up of the Eastern Gondwana Margin (New Zealand) documented by in-situ Zircon O–Hf Isotopes and Bulk-rock Sr–Nd Isotopes. Journal of Petrology. 59(5):849–880.

van der Pluijm BA, Hall CM, Vrolijk PJ, Pevear DR, Covey MC. 2001. The dating of shallow faults in the Earth's crust. Nature. 412:172–175. doi:10.1038/35084053.

Verma AR, Krishna P. 1966. Polymorphism and polytypism in crystals. New York: John Wiley and Sons.

Vermeesch P. 2018. Isoplotr: A free and open toolbox for geochronology. Geoscience Frontiers. 9(5):1479–1493.

Vrolijk P, van der Pluijm BA. 1999. Clay gouge. Journal of Structural Geology. 21:1039–1048.

York D, Evensen NM, Lopez Martinez M, De Basabe Delgado J. 2004. Unified equations for the slope, intercept, and standard errors of the best straight line. American Journal of Physics. 72:367–375.